# Towards a Virtual Keyboard Scheme Based on Wearing One Motion Sensor Ring on Each Hand

Chao Lian, Xianshou Ren, Yuliang Zhao, *Member, IEEE*, Xueliang Zhang, Ruoyu Chen, Shuyu Wang, Xiaopeng Sha, *Member, IEEE* and Wen J. Li, *Fellow, IEEE*

***Abstract*—In this paper, we present an improved ring-type virtual keyboard scheme that can achieve impressive performance with only one smart ring on a finger of each hand. The smart ring integrates a 6-DoF Inertial Measurement Unit (IMU) and a 3-DoF magnetometer sensor for collecting motion data during typing. First, a new keyboard layout is designed, by changing the previous rectangular layout to an arc structure, this method increases the difference in attitude angle between adjacent keys, which greatly improved the keystroke recognition accuracy. Secondly, other than the attitude angle feature, we also adopt acceleration data, gyroscope data and magnetometer data to describe the subtle differences between different keystrokes motion. Then, feature importance evaluation and feature correlation analysis were used to select features with high contribution rate and low similarity to describe keystrokes. Finally, nine effective features were selected from the attitude angle and magnetometer data for the final keystroke recognition. By weighing the number of selected features, recognition speed and recognition accuracy of training models, the keystroke recognition speed can increase by nearly 4 times while ensuring 98.53% of the keystroke recognition accuracy. This new ring-type virtual keyboard input scheme has the advantages in portability, small volume, and lower cost over many existing human-computer interface methods.**

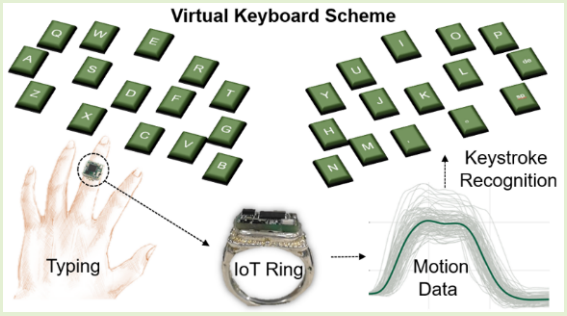


***Index Terms*—Internet of things, machine learning, virtual keyboard, wearable sensors, motion recognition.**

## I. Introduction

THE traditional QWERTY keyboard has been the most commonly used device for text input since 1971 [1]–[3], despite its problems such as poor portability, typing noise, and privacy leak. With the rapid development of human-computer interaction techniques, a variety of text input schemes have been developed. For example, the voice input method [4]–[6] has emerged as a popular choice for text input, which looks very natural and convenient. However, it struggles to identify the speaker in a noisy environment, and also brings inconvenience or even embarrassment when the user is in a quiet occasion. In addition, it also has problems with recognizing dialects and accents. As text input may occur in many occasions of our daily life, there is high requirement for the convenience of use of text input devices. Therefore, it is still a technical challenge to design a character input scheme which is accurate and portable enough to suit most of the user's requirements in daily life.

In recent years, researchers have proposed a number of virtual keyboard concepts and prototypes [7]–[22]. Compared to traditional keyboards, virtual keyboards can bring many advantages, such as portability, customizability and novelty. Nowadays, there are two primary types of virtual keyboards: ***non-contact virtual keyboard*** and ***wearable virtual keyboard***.

### A. The Non-Contact Virtual Keyboard

***The non-contact virtual keyboard*** often recognizes keystrokes by capturing motion data utilizing non-contact methods, such as laser, cameras. The laser-based keyboard utilizes the infrared technology to track the movements of fingers

Manuscript received August 15, 2020; accepted September 9, 2020. Date of publication September 14, 2020; date of current version January 6, 2021. This work was supported in part by the National Natural Science Foundation of China under Grant 61873307, in part by the Administration of Central Funds Guiding the Local Science and Technology Development under Grant 206Z1702G, in part by the Fundamental Research Funds for the Central Universities under Grant N2023015, in part by the Qinhuangdao Science and Technology Planning Project under Grant 201901B013, in part by the Hong Kong RGC-Joint Laboratory Funding Scheme under Grant JLFS/E-104/18, and in part by the Shenzhen Science and Technology Innovation Commission Municipality under Grant SGDX2019081623121725. The associate editor coordinating the review of this article and approving it for publication was Prof. Shih-Chia Huang. *(Chao Lian and Xianshou Ren contributed equally to this work.) (Corresponding authors: Yuliang Zhao; Wen J. Li.)*

Chao Lian, Xianshou Ren, Yuliang Zhao, Xueliang Zhang, Ruoyu Chen, Shuyu Wang, and Xiaopeng Sha are with the School of Control Engineering, Northeastern University at Qinhuangdao, Qinhuangdao 066004, China (e-mail: zhaoyuliang@neuq.edu.cn).

Wen J. Li is with the CAS-CityU Joint Laboratory on Robotics, Department of Mechanical Engineering, City University of Hong Kong, Hong Kong (e-mail: wenjli@cityu.edu.hk).

Digital Object Identifier 10.1109/JSEN.2020.3023964

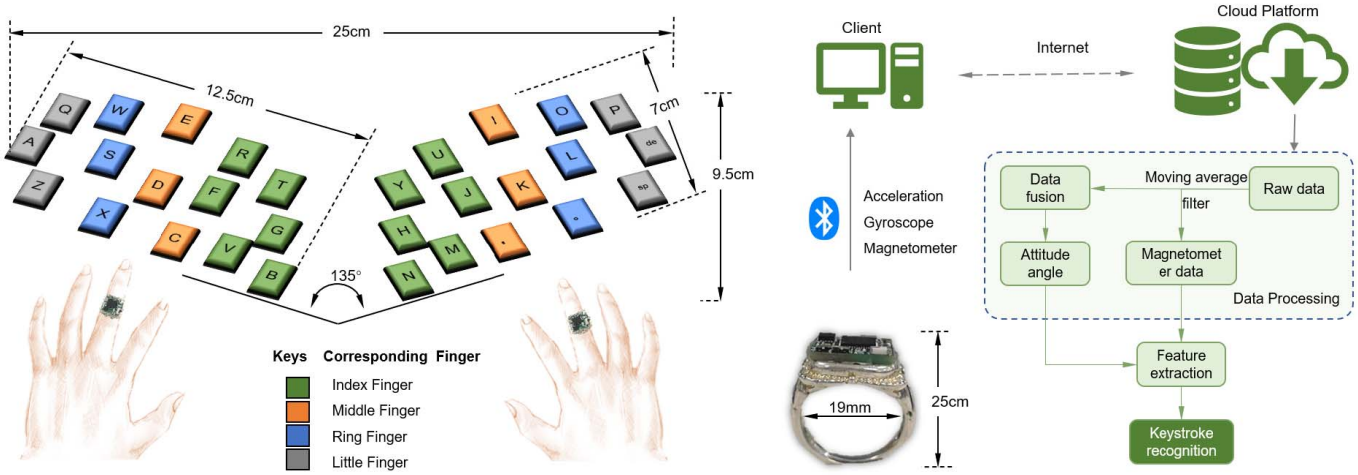


Fig. 1. (a) The layout of the keyboard and how the ring was worn during the original keystroke data collection process. (b) The flow chart of the experimental process.

and then predict the real input message [7]–[9]. This type of keyboard often requires the user to type on a smooth surface, and an unconscious contact during rest can lead to incorrect recognition. Kamran Ali *et al.* [10] firstly exploited the changes in channel state information (CSI) of WiFi signals for keystroke recognition. Unfortunately, this scheme is highly susceptible to variations in the environment such as human motion in surrounding areas, changes in orientation and distance of transceivers. The camera-based keyboard often uses the image processing technique to track finger motion and the location of the fingertip for precise identification [11]–[13]. However, changes in the tilt of the device placement would affect the camera's viewing angle, which impairs the accuracy of keystroke recognition.

### B. The Wearable Virtual Keyboard

***The wearable virtual keyboard*** usually uses a variety of sensors installed on the hands or wrists to detect the movements of palm muscles and fingers for keystroke recognition [14]–[20]. The "data glove" [15]–[19], integrating multiple sensors for finger gesture detection, is a common example. It can be used as a keyboard, mouse or other interactive device. However, it often has limitations on recognition accuracy, response time, and wearing comfortability. Another type of virtual input scheme is the hand-writing approach [21], which applies motion sensors to acquire motion trajectories or motion features for recognizing hand-written characters. There are also some other types of wearable virtual keyboards. The AirTouch [22] and VType [23] keyboards adopt the optical fiber in the glove to perform curvature detection on each keystroke when pressing a certain key. These two virtual keyboards offer a novel approach to keystroke detection, but with high costs and requiring circuit implementation. The Senseboard [24] keyboard, designed with two rubber pads, can detect muscle movements in the palm and translate them into keystrokes.

### C. Previous Work

In our previous work [25], [26], we proposed a ring-type virtual keyboard based on wearable IMU sensors. We discussed the impact of the number of sensors on keystroke recognition accuracy. The results showed that the recognition accuracy was extremely low when only one sensor was worn, which cannot meet the need for application, while wearing more than one sensor would make it inconvenient to type. Therefore, increasing the accuracy of keystroke recognition by wearing just one smart ring on each hand is a crucial step toward commercialization.

## II. Experimental Setup

### A. Experiment Platform

The QWERT keyboard layout has been widely adopted as the standard keyboard layout since 1971 [1]–[3]. To improve recognition accuracy, we designed a special layout for our ring-type virtual keyboard, which demonstrates the customizability of our scheme.

Fig. 1.a shows the keystroke layout template. It was printed on a A4 piece of paper, included 26 alphabet keys and four function keys (comma key, period key, space key, and delete key). The size of the keyboard layout was 25 cm × 9.5 cm. The left and right parts are symmetrically distributed, with an internal angle of 135 degrees and a size of 12.5 cm × 7 cm. Fifteen alphabets keys (Q, W, E, R, T, A, S, D, F, G, Z, X, C, V, and B) were regularly distributed on the left hand side. Similarly, eleven alphabets keys (Y, U, I, O, P, H, J, K, L, N, and M) and four function keys (comma key, period key, space key, and delete key) were distributed on the right side.

Fig. 1. b shows the lateral view of the smart ring. The smart ring [25] has a size of 19 mm × 16 mm × 25 mm and a weight of 7.8 grams (including a 5.3-gram ring structure, a 1.7-gram sensor board, and a 0.8-gram coin cell battery). It integrated a microprocessor (SoC Nrf52832), a 6-DoF inertial measurement sensor, a 3-DoF magnetometer sensor, and a coin cell battery. In the experiment, the sampling frequency was set to 50 Hz. The smart ring is powered by a 48mAh coin cell battery, which allows the ring to keep working for 8 consecutive hours. Meanwhile this system also has a sleeping mode and a turn on/off switch which can greatly reduce energy consumption during the spare time.

### B. Data Collection

The Home Row Keys were defined as the solid frames in Fig. 1.a. Before typing, users' fingers were placed on the Home Row Keys. As shown in Fig. 1.a, the ring was worn on the proximal phalanx of each hand, and each letter key was typed by a finger specific to the color of the key. For example, the left middle finger corresponds to the keys "E", "D", and "C". The assignment of keys can also be customized. Two subjects participated in the data collection. 100 sets of keystroke motion data were collected for each subject in 4 different times (25 sets per time). In each time, these 30 keys were typed in an order different from that in other times.

### C. Experiment Procedure

The whole keystroke recognition process is shown in Fig. 1.b. While pressing keys, the motion data (3-axis accelerometer data and 3-axis gyroscope data and 3-axis magnetometer data) would be collected by the IMU sensor and magnetometer sensor. Then, these data were transmitted to a client (phone or computer) through BLE. Subsequently, data processing, feature extraction and keystroke recognition would be performed. If computing resources were limited, these processes would be performed on the cloud platform.

## III. Data Processing

### A. Data Preprocessing

In the data preprocessing process, the moving average filter [27] was applied to eliminate the high-frequency noise of the collected keystroke motion data. The moving average filter algorithm is shown in (1).

$$y(i) = \frac{1}{M}\sum_{j=0}^{M-1} x[i-j] \tag{1}$$

where y is the output signal, and M is the size of the move window of the filter. The sliding window M can be adjusted to better eliminate the high-frequency noise.

Attitude angle can reflect the attitude of the smart ring relative to the ground using three Euler angles (yaw, pitch, and roll). It is more stable and accurate than acceleration and angular velocity in expressing keystroke motions. We calculated it by fusing the acceleration and gyroscope data using the angle complementary filter algorithm [28], as shown in (2).

$$\theta(k+1) = (1-\alpha) * a + \alpha * (\theta(k) + w * dt) \tag{2}$$

where $\theta$ is the attitude angle, a is the angle estimated by accelerometer data, w is the gyroscope data, $\theta$(k)+w∗dt is the angle estimated based on the measured gyroscope integration over time, and $\alpha$ is the weight coefficient, which is determined by (3).

$$\alpha = \frac{\tau}{\tau + dt} \tag{3}$$

where $\tau$ is the time constant.

When calculating the attitude angle, the integral effect would accumulate errors and affect the keystroke recognition accuracy. Thus, the average of the start point and end point values was subtracted from the corresponding attitude angle data. The mathematical description is shown in (4).

$$\theta_i = \theta_i - \frac{\theta_1 + \theta_n}{2}, \quad (i = 1, 2, 3, \ldots\ldots, n) \tag{4}$$

where $\theta$ is the final attitude angle data for each keystroke.

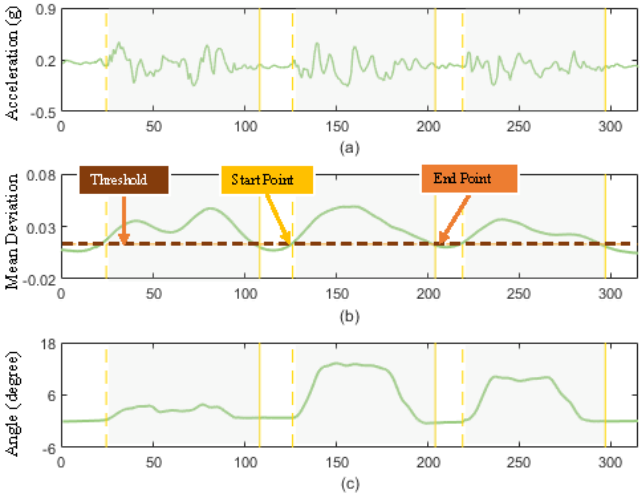


Fig. 2. (a) The waveform changes of acceleration data over time. (b) The waveform changes of MD over time. (c) The attitude angle of each keystroke segmentation.

### B. Keystroke Data Extraction

In this part, the motion data of each keystroke was extracted from the collected raw data. For convenience, this method was called the keystroke data extraction (KDE) algorithm, and described in detail in the following section.

As shown in Fig. 2.a, the keystroke motion signal (x-axis acceleration data) can be divided into active state and stationary state. Then, we framed the acceleration data and calculated the mean deviation (MD) in the sliding widow. The mathematical description of MD is described in (5) and (6).

$$\bar{x}_i = \frac{1}{L}\sum_{i=1}^{L} x_i(n) \tag{5}$$

$$MD = \frac{1}{L}\sum_{i}^{L} |x_i - \bar{x}_i| \tag{6}$$

The waveform changes of MD over time are shown in Fig. 2.b. The threshold $\alpha_{\text{th}}$ was used to detect the start and end points of the MD waveform. If MD (k) satisfies (7), the start point index for the keystroke segmentation can be obtained. Similarly, if MD (k) satisfies (8), the end point index can be obtained. In addition, keystroke completion may be misrecognized due to the hand shake and keystroke jitter, so threshold $\beta_{\text{th}}$ was used to indicate the hold time of the keystroke and limit the length of the data sampling window. If we define the start point as $k_1$ and the end point as $k_2$, the threshold of the keystroke window can be described in

formula (9).

$$\begin{cases} MD(k) < \alpha_{th} \\ MD(k+1) > \alpha_{th} \end{cases} \tag{7}$$

$$\begin{cases} MD(k) > \alpha_{th} \\ MD(k+1) < \alpha_{th} \end{cases} \tag{8}$$

$$k_2 - k_1 > \beta_{th} \tag{9}$$

In this way, as shown in Fig. 2.c, the attitude angle or raw data of each keystroke segmentation can be obtained. The experiment shows that it takes 12.1ms to recognize one keystroke when a computer with an Intel (R) Core (TM) i5-4210M CPU and 8 GB of main memory (RAM) is used.

## IV. Improvements and Results

In a previous work [25], the mean recognition accuracy with one wearable sensor worn on the middle finger was only 87.30%. To improve the recognition accuracy, three major improvements, which were intended to achieve high-precision keystroke recognition with just one smart ring worn on each hand, were made in this experiment.

### A. Self-Defined Keyboard Layout

Our previous experiment revealed that the difference in typing behaviors when using a traditional keyboard layout was not clearly distinguishable, which limited the recognition performance of our ring-type keyboard. By changing the previous rectangular layout to an arc structure, our proposed method increased the difference in attitude angle between adjacent keys, which greatly improved keystroke recognition accuracy. Meanwhile the distances between different keys were shortened to reduce hand fatigue. After the improvement, the mean accuracy increased from 87.30% to 95.73%, an increase of 8.43%. These results indicated that this layout design method enabled high-precision keystroke recognition.

To ensure better migration and application in different circumstances, we needed to consider not only the recognition accuracy, but also the universality of the algorithm. Thus, five universal machine learning classifiers, including decision tree (CART) [31], k-Nearest Neighbor (k-NN) [32], Naive Bayes (NB) [33], Support Vector Machine (SVM) [34], and Linear Discriminant Analysis (LDA) [35], were selected to perform keystroke classification and recognition. If the user follows the standard typing method, the established ML model will be a good choice. If the user's typing habit is far from the standard one, it will be necessary to train a new ML model. Additionally, training ML models will always help to improve the recognition accuracy of the user's typing. In addition, to reduce the effect of overfitting, non-crossing training data and test data were randomly selected in this experiment.

### B. Higher Dimensional Feature Description

Another improvement was made by feature mining, which aimed to find all the effective data for key expression. Six features, as listed in Table I, were extracted from the attitude angle data to describe keystrokes. Each feature contained different motion information. For example, the maximum value describes the strength of the keystroke, the average and median value represent the distribution level of keystroke data, and the standard variance reflects the dispersion degree of keystroke data. These statistical properties are suitable for motion classification and recognition, and have been widely used in machine learning algorithms [29], [30].

TABLE I
The Ten Features Selected to Describe Keystroke Motion

| Number | Name | Formula |
|---|---|---|
| 1 | Maximum value | $\text{Max} = max(x_i), i = 1,2,3,\ldots,n$ |
| 2 | Average value | $\text{Ave} = \frac{1}{n}\sum_{i=1}^{n} x_i$ |
| 3 | Standard variance | $\text{Std} = \sqrt{\frac{1}{n-1}\sum_{i=1}^{n}(x_i - \bar{x})^2}$, $\bar{x}=\frac{1}{n}\sum_{i=1}^{n} x_i$ |
| 4 | Midpoint value | $\text{Mid}=x[\frac{1}{2}(k_1+k_n)]$ |
| 5 | Median value | Median value of array |
| 6 | Short-term energy | $\text{Eng} = \sum_{i=1}^{n} x_i^2$ |

Subsequently, after repeated experimental studies, in addition to attitude angle data, we adopted the raw data (accelerometer, gyroscope and magnetometer data) for a synthetic representation of keys in a higher dimension. As shown in Fig. 3, three keys (A, B, and C) were selected as an example to show the stability and consistency of the raw keystroke data and attitude angle data. Each small graph includes 100 sets of keystroke motion data, and the blue line represents the average of these data sets. When typing a specific key, the waveform change trend of the keystroke data was consistent, and the waveform change trend of the motion of different keystrokes was significantly different. This indicated that these data showed very stable and unique performance when identifying different keystrokes. Therefore, simultaneously extracting features from the raw keystroke data and attitude angle data and describing keystrokes in a higher dimension could allow describing the subtle differences between different keystrokes.

Fig. 4 shows a comparison between the first and second improved results. The accuracy of the LDA classifier is increased by 4.53%, and the highest keystroke recognition accuracy is obtained at the same time, as high as 99.67%.

### C. Feature Optimization

In the above work, the keystroke recognition accuracy was increased with the first and second improvements. However, in the actual environment, the key recognition speed is a requirement that must be considered. Selecting effective features for keystroke recognition helps avoid heavy calculation workloads. There are several kinds of feature-importance-evaluation methods, such as Random Forest (RF) and Support Vector Machine (SVM). In most cases, RF is most likely to produce the best classification results [36]. The classification of RF was based on the "votes" of each tree, and the relative importance of each feature was measured by the

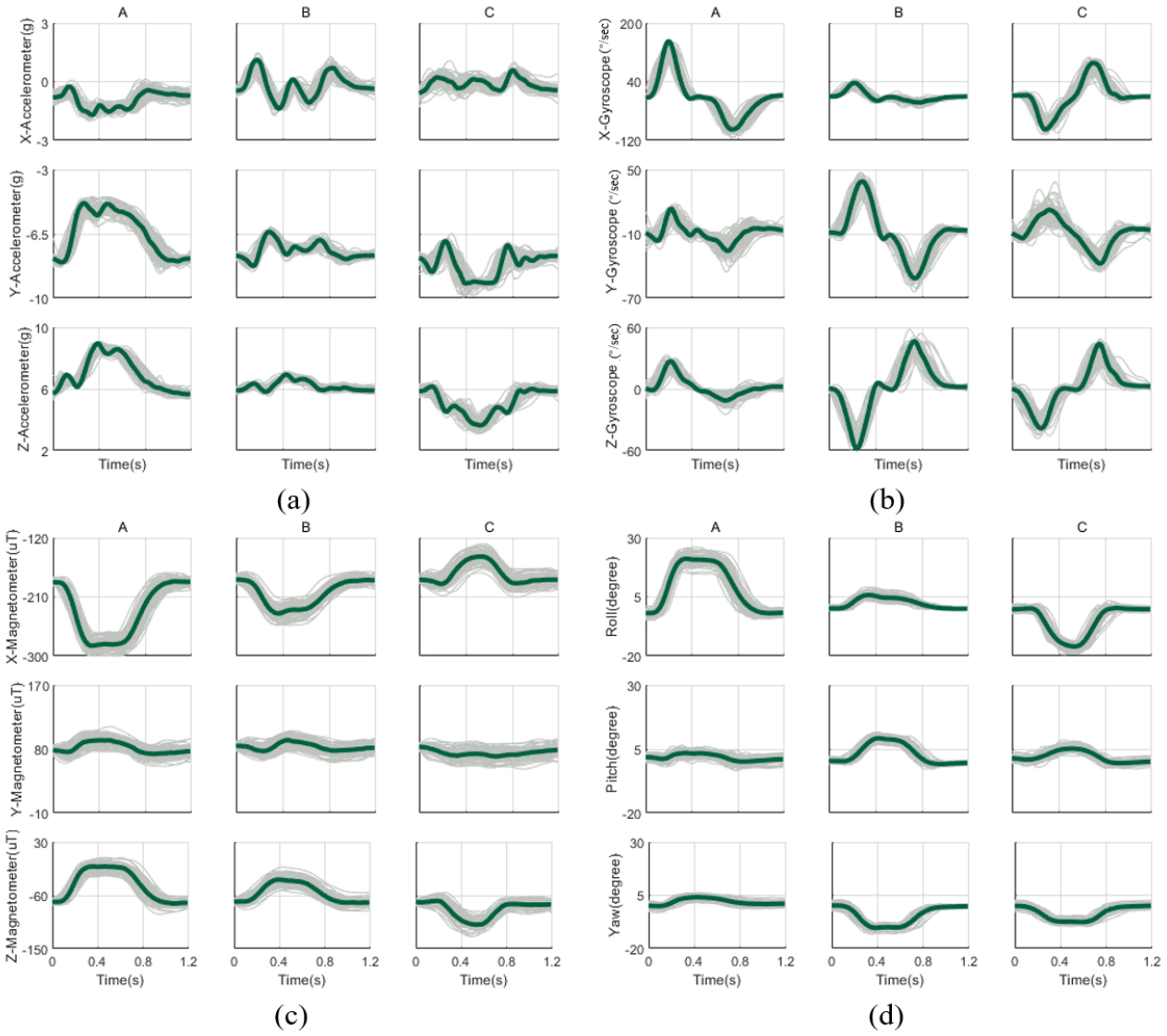


Fig. 3. (a) The waveform changes in the accelerometer data for keys “A”, “B” and “C”. (b) The waveform changes in the gyroscope data for keys “A”, “B” and “C”. (c) The waveform changes in the magnetometer data for keys “A”, “B” and “C”. (d) The waveform changes of attitude angle (roll, pitch, and yaw) for keys “A”, “B” and “C”.

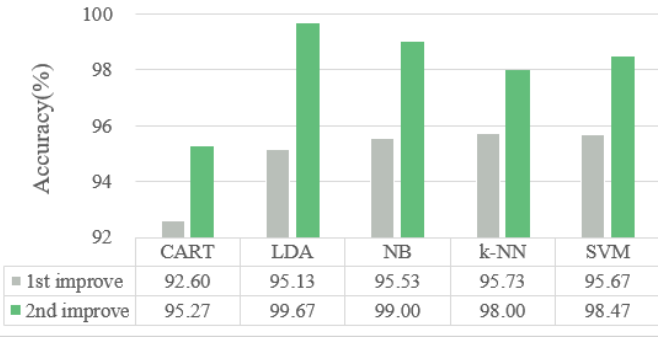


| | CART | LDA | NB | k-NN | SVM |
|---|---|---|---|---|---|
| 1st improve | 92.60 | 95.13 | 95.53 | 95.73 | 95.67 |
| 2nd improve | 95.27 | 99.67 | 99.00 | 98.00 | 98.47 |

Fig. 4. The results comparison between the first and second improvements.

Gini index [37]. The higher the Gini index of the feature, the greater the contribution of the feature to keystroke recognition accuracy.

In the second promotion, we selected 12 categories of keystroke data: 3-axis accelerometer, 3-axis gyroscope, 3-axis magnetometer, and pitch, yaw, and roll of attitude angle, with each category including six features (as shown in Table I). Fig. 5 shows the importance evaluation results of 72 features. Through statistical analysis, the top 40 features in the importance evaluation rank, with a cumulative contribution rate over 95%, were selected for keystroke recognition. In addition, if the similarity between two features is high, the effect they produce is equivalent to one feature, and additional features will increase the keystroke recognition time. After dropping out features with low contribution and high similarity, 29 features were selected from these 40 features. Finally, the similarity among these features is less than 98% and the Gini Index of high contribution is greater than 0.4%.

In the second promotion, the LDA classifier showed the best keystroke recognition accuracy. Therefore, as shown in Fig. 6, the LDA classifier was selected to describe the relationship between the keystroke recognition accuracy and the recognition time under different feature numbers. Here, the label

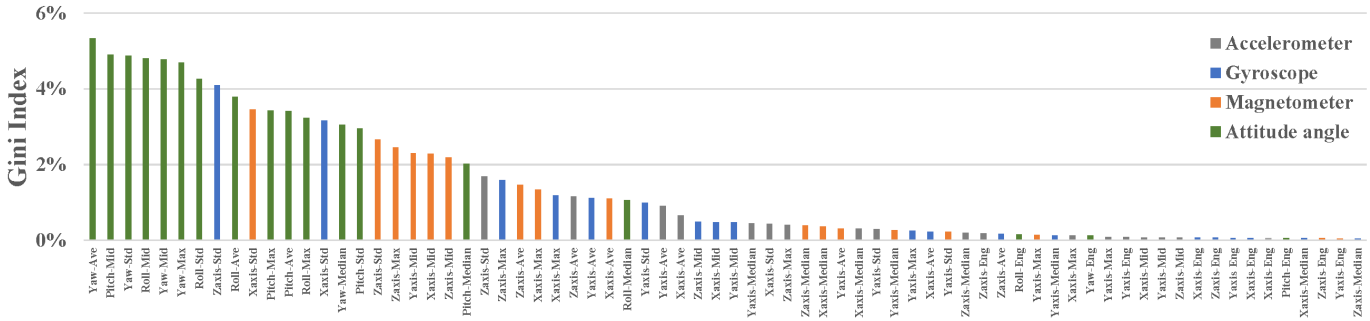


Fig. 5. Importance evaluation result of 72 features for keystroke data.

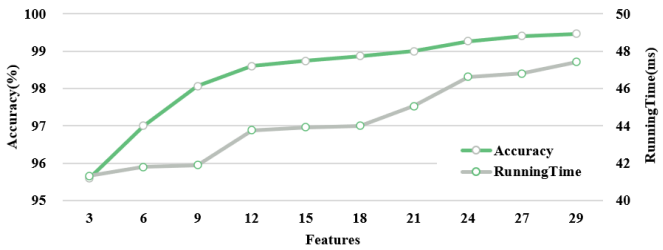


Fig. 6. The relationship between the number of features, keystroke recognition accuracy, and keystroke recognition time.

TABLE II
THE NINE FEATURES SELECTED TO DESCRIBE KEYSTROKE MOTION

| SN | Category | Feature |
|---|---|---|
| 1 | Attitude angle | Yaw-Ave |
| 2 | Attitude angle | Pitch-Mid |
| 3 | Attitude angle | Yaw-Std |
| 4 | Attitude angle | Yaw-Max |
| 5 | Attitude angle | Roll-Std |
| 6 | Magnetometer | Xaxis-Std |
| 7 | Attitude angle | Pitch-Max |
| 8 | Attitude angle | Pitch-Ave |
| 9 | Attitude angle | Roll-Max |

"3" indicates the three features with the highest contribution after feature importance ranking. By comparison and analysis, we found that the system delivers both high keystroke recognition accuracy and high recognition speed when nine features are selected. If additional features are added, the recognition accuracy is not prominent, but the running time is significantly increased. Therefore, nine features, as listed in Table II, were finally chosen for keystroke recognition.

## D. Results and Analysis

*1) Results of Three Improvements:* The results of the three improvements are listed in Table III. The classifiers SVM show better performance in the final keystroke recognition experiment. After completing these improvements, the recognition accuracy of each classifier was improved to different degrees.

TABLE III
KEYSTROKE RECOGNITION ACCURACY AFTER THREE MAJOR IMPROVEMENTS

| SN | CART | LDA | NB | k-NN | SVM |
|---|---|---|---|---|---|
| 1st improve | 92.60% | 95.13% | 95.53% | 95.73% | 95.67% |
| 2nd improve | 95.27% | 99.67% | 99.00% | 98.00% | 98.47% |
| 3rd improve | 96.00% | 98.07% | 98.20% | 98.53% | 98.67% |

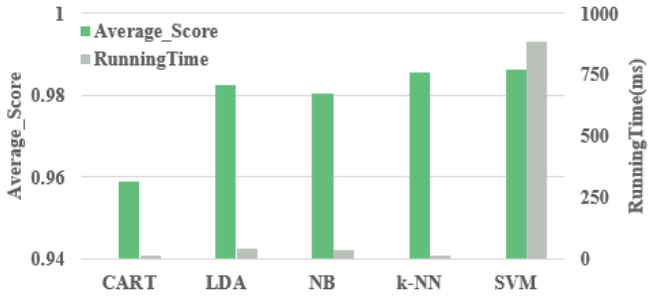


Fig. 7. The comparison of *Average_Score* and running time of keystroke recognition using different classifiers.

In each improvement, the ranking orders of the recognition accuracy of the five classifiers were not completely similar. This shows that after layout changes, optimal selection of features, and extraction of features from other dimensions (such as accelerometer, gyroscope, magnetometer, and attitude angle), it is necessary to compare the results of different machine learning algorithms and select the best algorithm for keystroke recognition.

*2) Performance Analysis:* In this section, in order to describe our experimental results in detail, we introduce precision, recall, F1-score, and confusion matrix to describe our experimental results. The mathematical description of the precision and recall involved in the confusion matrix can be described in formula (10) and (11).

$$Precision(m) = \frac{TP}{TP + FP} \tag{10}$$

$$Recall(m) = \frac{TP}{(TP + FN)} \tag{11}$$

here, m means different types of keystrokes, and the keystroke "A" was used as an example to describe the four parameters

**(a)**

Classified Values

| Actual Values \ Key | Q | W | E | R | T | A | S | D | F | G | Z | X | C | V | B | Recall (%) |
|---|---|---|---|---|---|---|---|---|---|---|---|---|---|---|---|---|
| Q | 97 | | | | | | | 1 | | | 2 | | | | | 97.00 |
| W | | 98 | 2 | | | | | | | | | | | | | 98.00 |
| E | | | 100 | | | | | | | | | | | | | 100.00 |
| R | | | | 100 | | | | | | | | | | | | 100.00 |
| T | | | | | 98 | | 2 | | | | | | | | | 98.00 |
| A | | | | | | 100 | | | | | | | | | | 100.00 |
| S | | | | | 2 | | 97 | | | 1 | | | | | | 97.00 |
| D | | | | | | | | 100 | | | | | | | | 100.00 |
| F | | | | | | | | | 100 | | | | | | | 100.00 |
| G | | | | | | | | | | 100 | | | | | | 100.00 |
| Z | 4 | | | | | | | 1 | | | 95 | | | | | 95.00 |
| X | | | | | | | | | 7 | | | 93 | | | | 93.00 |
| C | | | | | | | | | | | | | 100 | | | 100.00 |
| V | | | | | | | | | | | | | | 100 | | 100.00 |
| B | | | | | | | | | | | | | | | 100 | 100.00 |
| Precision(%) | 96.04 | 100.00 | 98.04 | 100.00 | 98.00 | 100.00 | 97.98 | 98.04 | 93.46 | 99.01 | 97.94 | 100.00 | 100.00 | 100.00 | 100.00 | |

**(b)**

Classified Values

| Actual Values \ Key | Y | U | I | O | P | H | J | K | L | Del | N | M | Com | Per | Spa | Recall (%) |
|---|---|---|---|---|---|---|---|---|---|---|---|---|---|---|---|---|
| Y | 100 | | | | | | | | | | | | | | | 100.00 |
| U | | 99 | 1 | | | | | | | | | | | | | 99.00 |
| I | | 2 | 98 | | | | | | | | | | | | | 98.00 |
| O | | | | 99 | 1 | | | | | | | | | | | 99.00 |
| P | | | | 1 | 99 | | | | | | | | | | | 99.00 |
| H | 1 | | | | | 99 | | | | | | | | | | 99.00 |
| J | | | | | | | 100 | | | | | | | | | 100.00 |
| K | | | | | | | | 100 | | | | | | | | 100.00 |
| L | | | | 1 | | | | | 99 | | | | | | | 99.00 |
| Del | | | | | 1 | | | | | 99 | | | | | | 99.00 |
| N | | | | | | | | | | | 95 | 5 | | | | 95.00 |
| M | | | | | | | | | | | 1 | 99 | | | | 99.00 |
| Com | | | | | | | | | | | | | 100 | | | 100.00 |
| Per | | | | | | | | | | | | | | 99 | 1 | 99.00 |
| Spa | | | | | | | | | | 1 | | | | 5 | 94 | 94.00 |
| Precision(%) | 99.01 | 98.02 | 98.99 | 98.02 | 98.02 | 100.00 | 100.00 | 100.00 | 100.00 | 99.00 | 98.96 | 95.19 | 100.00 | 95.19 | 98.95 | |

Fig. 8. (a) The result on the left-hand side by using the k-NN classifier. (b) The result on the right-hand side by using the k-NN classifier.

(TP, TN, FP, and FN) of the above formula. TP (true-positive) is correctly classified as "A". TN (true-negative) is correctly classified as not "A". FP (false-positive) is incorrectly classified as "A". FN (false-negative) is incorrectly classified as not "A".

First, the F1-Score of each keystroke recognition, defined in formula (12), was calculated. Then the *Average_Score* of each classification algorithm, defined in formula (13), was adopted as a comprehensive index of the algorithm's recognition performance.

$$F1\text{-}Score(m) = \frac{2 \times Precision(m) \times Recall(m)}{Precision(m) + Recall(m)} \quad (12)$$

$$Average\_Score = \frac{1}{n} \sum_{m=1}^{n} F1\text{-}Score(m) \quad (13)$$

Fig. 7 shows the comparison of *Average_Score* and time consuming of the keystroke recognition using different classifiers. We can see that the Score of CART is the smallest, less than 0.96, while the k-NN and SVM classifiers ensure a high Score, both of which exceed 0.98. However, the running times of k-NN and SVM classifiers are 12.0536ms and 884.32ms, respectively. When the Score difference between k-NN and SVM is very small, the running speed of k-NN exceeds 73 times of SVM. Therefore, we choose k-NN as the final keystroke recognition. In addition, the running speed of k-NN is almost 4 times that of LDA selected in the second improvement.

In order to show our results, the confusion matrix [38] was introduced to describe the experimental results in detail. For a particular keystroke, the diagonal elements of the confusion matrix represent the correctly predicted keystrokes. The total number of diagonal elements represents the number of correctly predicted categories. Fig.8 shows the confusion matrix for keystroke recognition using the k-NN model. Take the key "Q" in Fig. 8(a) as an example. In the first column, the classified values of the key "Q" is 101 (97 + 4). Among them, the correct classification is 97 times, and the incorrect classification is 4 times (4 times "Z"), so the precision ("Q") is 96.04% (97/101). In the first row, the actual values of the key "Q" is 100 (97+1+2). Among them, the correct classification is 97 times, and the incorrect classification is 3 times (1 time "D", 2 times "Z"), so the recall rate ("Q") is 97% (97/100).

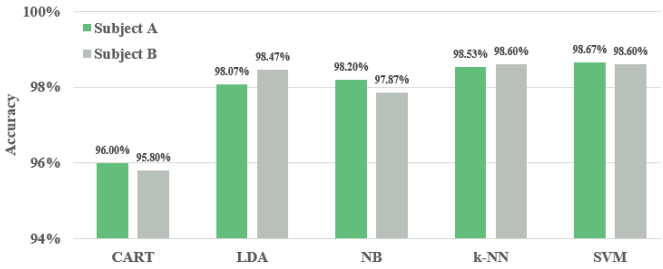


Fig. 9. The comparison of keystroke recognition accuracy of different subjects and classifiers.

Fig. 9 shows that the influence of different subjects on the recognition accuracy is much smaller than that of different recognition algorithms.

## V. Conclusion

We accurately recognized keystrokes by wearing just one smart ring on a finger of each hand during typing. This is a promising result for potentially wide utilization of our virtual keyboard scheme in real-life applications.

Compared to our previous works on ring-type keyboards, three major advancements were made to improve the recognition accuracy and recognition speed. Firstly, a new keyboard layout is designed. By changing the previous rectangular layout to an arc structure, this method increases the difference in attitude angle between adjacent keys, which greatly improved the keystroke recognition accuracy. Meanwhile the distances between different keys were shorten to reduce hand fatigue. The results show that the mean accuracy increased from

87.30% to 95.73%, an increase of 8.43%. Secondly, the subtle differences of different keys were described from a higher dimension. And it can describe each key more sufficient. Thirdly, feature importance evaluation and feature correlation analysis were used for feature optimization, which avoids heavy computational workload while ensuring the speed and accuracy. Finally, nine features that describe keystroke motion and the k-NN classifier that provides high accuracy, fast recognition, and much more simplicity, was selected to perform keystroke recognition.

In the future, by providing a personalized module to learn personal typing habits, it will help improve the accuracy of keystroke recognition. To further reduce the keystroke misrecognition rate, it is also feasible to arrange the frequently used keys on easily recognizable positions.

## REFERENCES


[1] K. Jasmin and D. Casasanto, "The QWERTY effect: How typing shapes the meanings of words," *Psychonomic Bull. Rev.*, vol. 19, no. 3, pp. 499–504, Jun. 2012.

[2] J. Noyes, "The QWERTY keyboard: A review," *Int. J. Man. Mach. Stud.*, vol. 18, no. 3, pp. 265–281, 1983.

[3] L. U. Ya-Jun, "A study of layout and input method of a genenal Tibetan computer keyboard," *J. Chinese Inf. Process.*, vol. 20, no. 2, pp. 78–86, 2006.

[4] O. Abdel-Hamid, A.-R. Mohamed, H. Jiang, L. Deng, G. Penn, and D. Yu, "Convolutional neural networks for speech recognition," *IEEE/ACM Trans. Audio, Speech Language Process.*, vol. 22, no. 10, pp. 1533–1545, Oct. 2015.

[5] M. G. Elfeky, P. Moreno, and V. Soto, "Multi-dialectical languages effect on speech recognition too much choice can hurt," *Procedia Comput. Sci.*, vol. 128, pp. 1–8, 2018, doi: 10.1016/j.procs.2018.03.001.

[6] H. Kwon, Y. Kim, H. Yoon, and D. Choi, "Selective audio adversarial example in evasion attack on speech recognition system," *IEEE Trans. Inf. Forensics Security*, vol. 15, pp. 526–538, 2020, doi: 10.1109/TIFS.2019.2925452.

[7] L. Chittaro and R. Sioni, "An electromyographic study of a laser pointer-style device vs. mouse and keyboard in an object arrangement task on a large screen," *Int. J. Hum.-Comput. Stud.*, vol. 70, no. 3, pp. 234–255, Mar. 2012.

[8] J. Cook, "Bluetooth virtual keyboard—A real taste of virtual reality!" *Pocket Pc*, vol. 8, no. 3, p, pp. 42–43, 2005.

[9] X. Wang and A. Hedge, "A usability evaluation of a laser projection virtual keyboard," in *Proc. Hum. Factors Ergonomic Soc. Annu. Meeting*, 2008, pp. 537–541.

[10] K. Ali, A. X. Liu, W. Wang, and M. Shahzad, "Recognizing keystrokes using WiFi devices," *IEEE J. Sel. Areas Commun.*, vol. 35, no. 5, pp. 1175–1190, May 2017.

[11] A. Bellino and V. Herskovic, "CameraKeyboard: A novel interaction technique for text entry through smartphone cameras," *IEEE Access*, vol. 7, pp. 167982–167996, 2019.

[12] J. Hu, G. Li, X. Xie, Z. Lv, and Z. Wang, "Bare-fingers touch detection by the button's distortion in a projector–camera system," *IEEE Trans. Circuits Syst. Video Technol.*, vol. 24, no. 4, pp. 566–575, Apr. 2014.

[13] Y. Yin, Q. Li, L. Xie, S. Yi, E. Novak, and S. Lu, "CamK: Camera-based keystroke detection and localization for small mobile devices," *IEEE Trans. Mobile Comput.*, vol. 17, no. 10, pp. 2236–2251, Oct. 2018.

[14] E. Arkenbout, J. de Winter, and P. Breedveld, "Robust hand motion tracking through data fusion of 5DT data glove and nimble VR kinect camera measurements," *Sensors*, vol. 15, no. 12, pp. 31644–31671, Dec. 2015.

[15] B. Fang, F. Sun, H. Liu, and C. Liu, "3D human gesture capturing and recognition by the IMMU-based data glove," *Neurocomputing*, vol. 277, pp. 198–207, Feb. 2018.

[16] S. S. Fels and G. E. Hinton, "Glove-talk: A neural network interface between a data-glove and a speech synthesizer," *IEEE Trans. Neural Netw.*, vol. 4, no. 1, pp. 2–8, Jan. 1993.

[17] P.-C. Hsiao, S.-Y. Yang, B.-S. Lin, I.-J. Lee, and W. Chou, "Data glove embedded with 9-axis IMU and force sensing sensors for evaluation of hand function," in *Proc. 37th Annu. Int. Conf. IEEE Eng. Med. Biol. Soc. (EMBC)*, Aug. 2015, pp. 4631–4634.

[18] B.-S. Lin, P.-C. Hsiao, S.-Y. Yang, C.-S. Su, and I.-J. Lee, "Data glove system embedded with inertial measurement units for hand function evaluation in stroke patients," *IEEE Trans. Neural Syst. Rehabil. Eng.*, vol. 25, no. 11, pp. 2204–2213, Nov. 2017.

[19] R. Shi, Z. Lou, S. Chen, and G. Shen, "Flexible and transparent capacitive pressure sensor with patterned microstructured composite rubber dielectric for wearable touch keyboard application," *Sci. China Mater.*, vol. 61, no. 12, pp. 1587–1595, Dec. 2018.

[20] S. Takamatsu, T. Lonjaret, E. Ismailova, A. Masuda, T. Itoh, and G. G. Malliaras, "Wearable keyboard using conducting polymer electrodes on textiles," *Adv. Mater.*, vol. 28, no. 22, pp. 4485–4488, 2016.

[21] S. Khan, H. Ali, Z. Ullah, N. Minallah, S. Maqsood, and A. Hafeez, "KNN and ANN-based recognition of handwritten pashto letters using zoning features," *Int. J. Adv. Comput. Sci. Appl.*, vol. 9, no. 10, pp. 1–9, 2018.

[22] C.-H. Ting, T.-H. Jen, C.-H. Chen, H.-P.-D. Shieh, and Y.-P. Huang, "3D air-touch user interface with high touch accuracy on stereoscopic displays," *J. Display Technol.*, vol. 12, no. 5, pp. 429–434, May 2016.

[23] C. Zeh *et al.*, "Polarization mode preservation in elliptical index tailored optical fibers for apertureless scanning near-field optical microscopy," *Appl. Phys. Lett.*, vol. 97, no. 10, pp. 1–3, 2010.

[24] F. B. D. Medeiros, F. Davin, A. Barros, and R. Dantas, "Senseboard: A touchless input device for hand motion detection," in *Proc. 20th Symp. Virtual Augmented Reality (SVR)*, Oct. 2018, pp. 248–252.

[25] Y. Zhao, C. Lian, X. Zhang, X. Sha, G. Shi, and W. J. Li, "Wireless IoT motion-recognition rings and a paper keyboard," *IEEE Access*, vol. 7, pp. 44514–44524, 2019.

[26] X. Sha, C. Lian, Y. Zhao, J. Yu, S. Wang, and W. J. Li, "An explicable keystroke recognition algorithm for customizable ring-type keyboards," *IEEE Access*, vol. 8, pp. 22933–22944, 2020.

[27] S. Golestan, M. Ramezani, J. M. Guerrero, F. D. Freijedo, and M. Monfared, "Moving average filter based phase-locked loops: Performance analysis and design guidelines," *IEEE Trans. Power Electron.*, vol. 29, no. 6, pp. 2750–2763, Jun. 2014.

[28] V. Kubelka and M. Reinstein, "Complementary filtering approach to orientation estimation using inertial sensors only," in *Proc. IEEE Int. Conf. Robot. Autom.*, May 2012, pp. 599–605.

[29] D. Figo, P. C. Diniz, D. R. Ferreira, and J. M. P. Cardoso, "Preprocessing techniques for context recognition from accelerometer data," *Pers. Ubiquitous Comput.*, vol. 14, no. 7, pp. 645–662, Oct. 2010.

[30] J. Wannenburg and R. Malekian, "Physical activity recognition from smartphone accelerometer data for user context awareness sensing," *IEEE Trans. Syst., Man, Cybern. Syst.*, vol. 47, no. 12, pp. 3142–3149, Dec. 2017.

[31] W. R. Burrows, M. Benjamin, S. Beauchamp, E. R. Lord, D. McCollor, and B. Thomson, "CART decision-tree statistical analysis and prediction of summer season maximum surface ozone for the Vancouver, Montreal, and Atlantic regions of Canada," *J. Appl. Meteorol.*, vol. 34, no. 8, pp. 1848–1862, Aug. 1995.

[32] M. R. Kolahdouzan and C. Shahabi, "Voronoi-based K nearest neighbor search for spatial network databases," in *Proc. VLDB Conf.*, 2004, pp. 840–851.

[33] T. Calders and S. Verwer, "Three Naive Bayes approaches for discrimination-free classification," *Data Mining Knowl. Discovery*, vol. 21, no. 2, pp. 277–292, Sep. 2010.

[34] G. Orrù, W. Pettersson-Yeo, A. F. Marquand, G. Sartori, and A. Mechelli, "Using support vector machine to identify imaging biomarkers of neurological and psychiatric disease: A critical review," *Neurosci. Biobehavioral Rev.*, vol. 36, no. 4, pp. 1140–1152, Apr. 2012.

[35] X. Jin, M. Zhao, T. W. S. Chow, and M. Pecht, "Motor bearing fault diagnosis using trace ratio linear discriminant analysis," *IEEE Trans. Ind. Electron.*, vol. 61, no. 5, pp. 2441–2451, May 2014.

[36] L. Ma *et al.*, "Evaluation of feature selection methods for object-based land cover mapping of unmanned aerial vehicle imagery using random forest and support vector machine classifiers," *ISPRS Int. J. Geo-Inf.*, vol. 6, no. 2, p. 51, Feb. 2017.

[37] R. I. Lerman and S. Yitzhaki, "A note on the calculation and interpretation of the Gini index," *Econ. Lett.*, vol. 15, nos. 3–4, pp. 363–368, Jan. 1984.

[38] O. Caelen, "A Bayesian interpretation of the confusion matrix," *Ann. Math. Artif. Intell.*, vol. 81, nos. 3–4, pp. 429–450, Dec. 2017.

**Chao Lian** received the B.E. degree from Liaoning Technical University in 2017. He is currently pursuing the M.S. degree with the School of Control Engineering, Northeastern University at Qinhuangdao, China. His current research interests are in the areas of wearable cyber physical devices, inertial measurement unit, motion analysis, machine learning, and artificial intelligence.

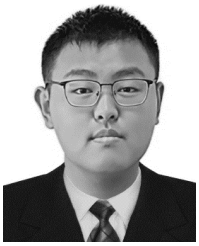

**Xianshou Ren** received the B.E. degree from the University of Jinan in 2019. He is currently pursuing the M.S. degree with the School of Control Engineering, Northeastern University at Qinhuangdao, China. His current research interests are in the areas of machine learning, data fusion, wearable device, and pattern recognition.

**Yuliang Zhao** (Member, IEEE) received the B.S. degree in mechanical engineering from the Hubei University of Automotive Technology, the M.S. degree in mechanical engineering from Northeastern University, and the Ph.D. degree in mechanical and biomedical engineering from the City University of Hong Kong in 2016. He is currently an Assistant Professor with the Northeastern University at Qinhuangdao, Qinhuangdao, China. His research interests include intelligent sensors, machine learning, motion analytics, and big data analyses; his recent work involves applying these technologies to sports and biomechanical analyses.

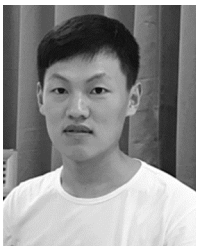

**Xueliang Zhang** received the B.S. degree in automation from Qingdao Technological University in 2018. He is currently pursuing the master's degree in control engineering with Northeastern University at Qinhuangdao, Qinhuangdao, China. His research interests include intelligent wearable devices, inertial measurement units, and cyber physical systems.

**Ruoyu Chen** is currently pursuing the B.E. degree with the School of Control Engineering, Northeastern University at Qinhuangdao, China. His current research interests are in the areas of deep learning, pattern recognition, and computer vision.

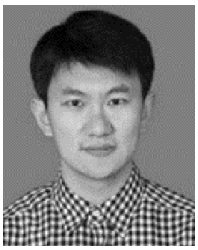

**Shuyu Wang** received the B.S. degree in mechanical engineering from the Huazhong University of Science and Technology, in 2013, and the Ph.D. degree in mechanical engineering from Stony Brook University (SUNY), in 2017. He is currently an Associate Professor with the Control Engineering Department, Northeastern University at Qinhuangdao, China. He has semiconductor industry experience with Global-Foundries. His current research interest includes biosensing and machine learning's applications in sensing.

**Xiaopeng Sha** (Member, IEEE) received the M.S. degree from the Department of Information Engineering, Tangshan College, and the Ph.D. degree from the School of Electrical Engineering, Yanshan University, China. She is currently a Lecturer with Northeastern University at Qinhuangdao. Her research interests include micro visual servoing, microrobotic systems, and intelligent sensors.

**Wen J. Li** (Fellow, IEEE) received the B.S. and M.S. degrees in aerospace engineering from the University of Southern California (USC), in 1987 and 1989, respectively, and the Ph.D. degree in aerospace engineering from the University of California, Los Angeles (UCLA), in 1997. He is currently a Chair Professor with the Department of Mechanical Engineering, and concurrently serving as an Associate Provost (Institutional Initiatives) of the City University of Hong Kong. From September 1997 to October 2011, he was with the Department of Mechanical and Automation Engineering, The Chinese University of Hong Kong. His industrial experience includes the Aerospace Corporation, El Segundo, CA, NASA Jet Propulsion Laboratory, Pasadena, CA, and Silicon Microstructures, Inc., Fremont, CA. His current research interests include intelligent cyber physical sensors, super-resolution microscopy and nanoscale sensing and manipulation. Dr. Li is the President of the IEEE Nanotechnology Council in 2016 and 2017.